

Geophysical Research Letters

RESEARCH LETTER

10.1029/2020GL091823

Key Points:

- Local observations can be used to constrain the intensity distribution of precipitation events associated with different synoptic systems
- The constraints allow projecting extreme return levels at scales relevant for impact studies from synoptic information from climate models
- The approach improves the predictability of local extremes, independent of improvements in climate models at regional and local scales

Supporting Information:

- Supporting Information S1

Correspondence to:

F. Marra,
f.marra@isac.cnr.it








Citation:

Marra, F., Armon, M., Adam, O., Zoccatelli, D., Gazal, O., Garfinkel, C. I., et al. (2021). Towards narrowing uncertainty in future projections of local extreme precipitation. *Geophysical Research Letters*, 48, e2020GL091823. <https://doi.org/10.1029/2020GL091823>

Received 30 NOV 2020

Accepted 23 JAN 2021

Toward Narrowing Uncertainty in Future Projections of Local Extreme Precipitation

Francesco Marra^{1,2} , Moshe Armon¹ , Ori Adam¹ , Davide Zoccatelli¹, Osama Gazal³ , Chaim I. Garfinkel¹ , Dorita Rostkier-Edelstein^{1,4}, Uri Dayan⁵, Yehouda Enzel¹ , and Efrat Morin¹ 

¹The Fredy and Nadine Herrmann Institute of Earth Sciences, The Hebrew University of Jerusalem, Jerusalem, Israel, ²Institute of Atmospheric Sciences and Climate, National Research Council of Italy, CNR-ISAC, Bologna, Italy, ³Faculty of Agricultural and Environmental Sciences, Szent Istvan University, Godollo, Karoly, Hungary, ⁴Department of Environmental Physics, Environmental Sciences Division, IIBR, Ness-Ziona, Israel, ⁵Department of Geography, The Hebrew University of Jerusalem, Jerusalem, Israel

Abstract Projections of extreme precipitation based on modern climate models suffer from large uncertainties. Specifically, unresolved physics and natural variability limit the ability of climate models to provide actionable information on impacts and risks at the regional, watershed and city scales relevant for practical applications. Here, we show that the interaction of precipitating systems with local features can constrain the statistical description of extreme precipitation. These observational constraints can be used to project local extremes of low yearly exceedance probability (e.g., 100-year events) using synoptic-scale information from climate models, which is generally represented more accurately than the local scales, and without requiring climate models to explicitly resolve extremes. The novel approach, demonstrated here over the south-eastern Mediterranean, offers a path for improving the predictability of local statistics of extremes in a changing climate, independent of pending improvements in climate models at regional and local scales.

Plain Language Summary Climate change impact studies are currently restrained by the limited accuracy of climate models in resolving precipitation extremes, by the computational power required to run high-resolution models, and by the uncertainties characterizing their analysis. Here, we present a novel approach which permits to project extreme precipitation for future climatic scenarios based on the combination of coarse-scale information from climate models with local observations. Focusing on the south-eastern Mediterranean, we provide projections of precipitation extremes which could not yet be derived using traditional methods, such as the events occurring on average once in 100 years. The combined effect of changes in intensity and occurrence of two dominant synoptic systems is projected to increase the intensity of the 100-year events in the coast and in the desert areas of the region and to decrease it elsewhere. The novel approach offers a path for improving the predictability of extremes in a changing climate, independent of pending improvements in climate models.

1. Introduction

In recent decades, natural hazards associated with extreme precipitation, such as floods and landslides, claimed thousands of lives and billions of US\$ in damages every year (NOAA, 2020; Paprotny et al., 2018). These numbers are expected to grow in response to an expansion of population and wealth toward hazard-prone areas and to modifications in the hydrological cycle induced by climate change (Ceola et al., 2014; Fischer & Knutti, 2016; Winsemius et al., 2016). Quantifying climate change impact on extremes is thus a major challenge for the research community (Blöschl et al., 2019). Hydrological design and risk management, particularly relevant for adaptation efforts, require information on low yearly exceedance probabilities (Chow et al., 1988), such as the events exceeded on average once in 100 years (hereon 100-year return levels, with 1% yearly exceedance probability). To directly quantify return levels, long data series are required, several times longer than the exceedance probability time scale. Since observational records rarely exceed 50–100 years, some form of statistical extrapolation is generally required (Coles, 2001).

Earth system models (ESMs) commonly guide impact studies. However, modern ESMs, used to simulate future-climate scenarios, are unable to explicitly resolve convective and microphysical processes critical

for precipitation extremes, and rely instead on parameterizations (Wilcox & Donner, 2007). Additionally, their output is most relevant at scales which are too coarse for many practical applications (Fischer et al., 2013; Hausfather et al., 2019). High-resolution dynamical downscaling methods can resolve convective processes and can thus provide accurate projections of local extreme precipitation for a region of interest (Prein et al., 2020). However, the applicability of these models is limited by heavy computational requirements. Currently, only few regions are covered with 10–20-year simulations (Fosser et al., 2020; Kendon et al., 2014), too short to reliably estimate 10-year return levels, let alone 100-year events. Furthermore, convection-permitting models are sensitive to boundary conditions from ESMs (Keller et al., 2018; Shepherd, 2014); thus understanding the mechanisms behind observed changes requires sensitivity analyses, which are still computationally unfeasible. Strategies to exploit the available model runs are thus needed to reach even a minimal level of accuracy for, say, 100-year events (e.g., Kelder et al., 2020).

Alternatively, statistical models can be combined with variables that are strongly related to extreme precipitation but more reliably reproduced in ESMs, such as temperature (Pfahl et al., 2017; Sippel et al., 2015). The methods currently adopted to quantify return levels, however, heavily rely on extremes, such as the maxima values in each year or the values exceeding high thresholds (Coles, 2001). As these are rare and subject to large stochastic uncertainties, the applicability of such methods in a changing climate is limited (Serinaldi & Kilsby, 2015; Tabari, 2021). In fact, stochastic climate variability sets a lower bound on the uncertainty in observed and modeled extremes (Fatichi et al., 2016).

This paper presents a novel statistical approach that avoids the stochastic uncertainties characterizing extremes and, relying on the understanding of the underlying processes, permits computationally efficient estimates of future return levels. It is shown here that the interaction of precipitating systems with local features, such as coastlines or orography, can constrain the statistical description of precipitation intensity. These constraints, derived from in situ observations, permit predicting future extreme return levels at the local scales based on coarse-resolution global climate model projections and without requiring models to explicitly resolve the extremes.

2. Study Area and Data

The south-eastern Mediterranean is regarded as a climate change hotspot, highly vulnerable to water scarcity and precipitation-induced hazards (Alpert et al., 2002; Giorgi, 2006). Strong spatial gradients in precipitation climatology (Figures S1 and S2 in the Supporting Information) emerge from the interactions of two main types of precipitating systems with coastline and orography (Figure 1a) (Diskin, 1970): (i) low-pressure systems moving inland along westerly tracks (Mediterranean cyclones, hereon *Type-1*) and (ii) low-pressure systems mainly extending from the south (active Red Sea troughs, *Type-2*). These are characterized by distinct spatial patterns and both yield extreme precipitation amounts (Armon et al., 2018; Marra, Zoccatelli, et al., 2019). ESMs predict substantial changes in the intensity and occurrence frequency of both systems (Hochman, Harpaz, et al., 2018; Hochman, Mercogliano, et al., 2018; Zappa et al., 2015), implying nonlinear changes in the compound extremes, which can be further complicated by local effects.

2.1. Precipitation Data

Daily precipitation data, summed up to 6:00UTC, were provided by the Ministry of Water and Irrigation of Jordan (97 stations between 1980–1981 and 2017–2018) and the Israel Meteorological Service (>1,300 stations between 1948–1949 and 2017–2018). Data from Israeli stations flagged as missing, inaccurate, interpolated, or obtained from multiday accumulations were excluded from the analysis. Jordanian data were supplied with no quality indicators; we therefore rely on quality controls by the data provider. Separate records measured in proximity of up to 1 km distance and 50 m elevation were merged. Records were organized by hydrologic years (September 1 to August 31). For each station, years with more than 14 unavailable days and records with less than 30 hydrological years were discarded. The final data set consists of 459 stations (404 from Israel, 55 from Jordan, average spatial density of $\sim 1/75 \text{ km}^{-2}$) with 30–70 complete years of record (50.1 ± 13.3 years). Stationarity of the annual maxima at each station is ensured using the Phillips and Perron (1988) test (5% significance level), indicating that the data adequately represent extremes under present conditions.

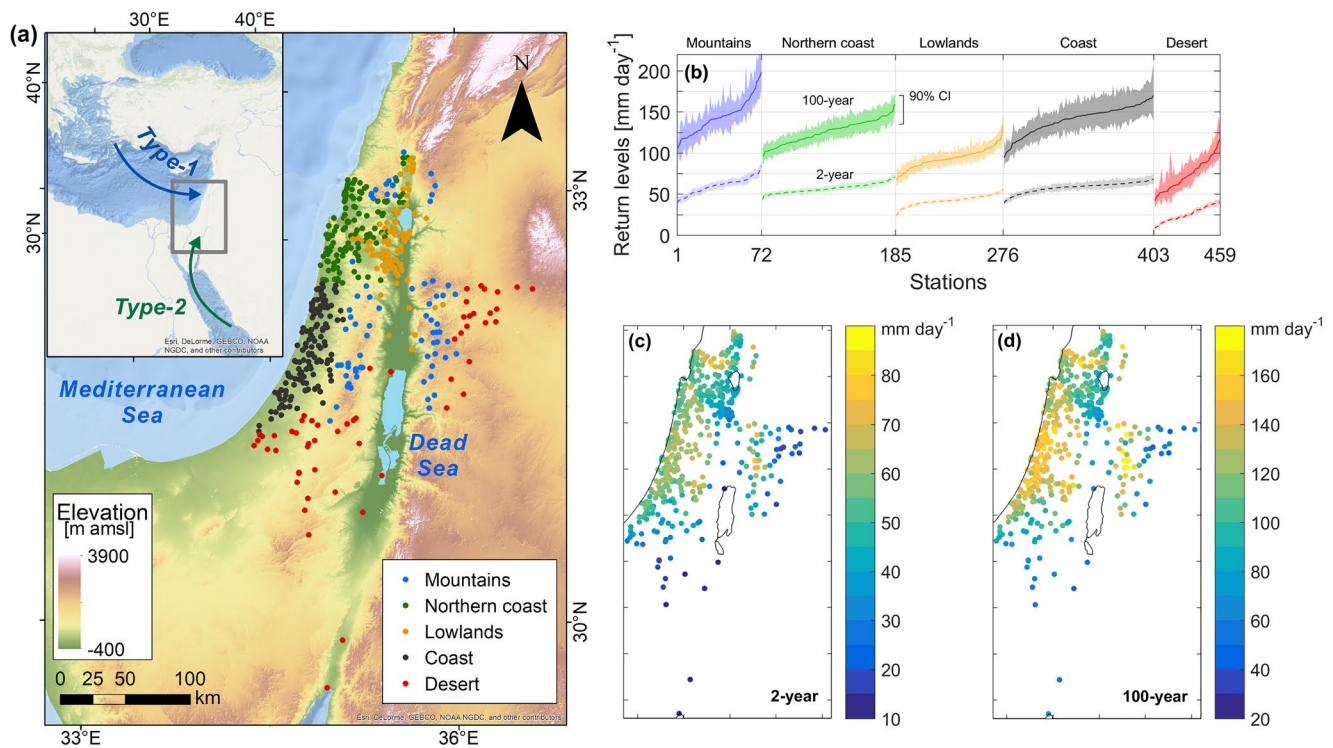


Figure 1. Extremes emerge from the interaction of precipitating systems with local features. (a) Map of the study region showing the local terrain elevation, the main precipitating systems tracks, and the location of the daily precipitation stations used in the study, colored according to groups in which different local features dominate the interaction with the precipitating systems. (b) Distribution of 2-year and 100-year return levels (50% and 1% yearly exceedance probability, respectively) of the five groups shown in (a) (with matching colors) displayed as transposed cumulative distributions. The respective uncertainty (shading) is calculated as the 90% confidence interval from 10^3 bootstrap samples with replacement among the years in the record. The median uncertainty across all groups is 14% (22%) for 2-year (100-year) return levels. (c, d) Map of the 2-year (c) and 100-year (d) return levels (colors indicate daily precipitation intensity).

2.2. Local Groups of Stations

Groups of stations in which distinct local features dominate the interaction with the precipitating systems are identified using a *k*-means clustering algorithm based on geographical (latitude, longitude, and elevation) and precipitation (average wet-day amount, and standard deviation of the wet-day amounts) properties, without any direct use of extreme precipitation properties or classification of the precipitating systems. The variables are normalized to zero-mean equi-dispersed distributions; the algorithm is iterated 99 times to ensure stable results. Following the Calinski and Harabasz (1974) criterion, six groups are obtained, roughly identifiable as mountains, northern coast, lowlands, coast, deserts west of the Dead Sea rift, and deserts east of the rift. The last two groups are characterized by similar climatic conditions and are likely separated primarily due to the geographical distance, although differences in other aspects may exist, such as elevation and distance from the sea. These two groups, which are sparsely populated (only 21 stations in one group), were merged. The classification used in the analysis consists of five groups: mountains, northern coast, lowlands, coast, and deserts (Figure 1a).

3. Methods

Extreme precipitation events were shown to emerge from underlying distributions of ordinary events (Marani & Ignaccolo, 2015; Zorzetto et al., 2016), whose tails are generally described by two parameters (e.g., stretched-exponential or power-type) (Cavanaugh et al., 2015; Marra, Borga, et al., 2020; Papalexioiu et al., 2018). By relying on ordinary events, for which more data are available, this approach decreases the stochastic uncertainties inherent in the realization of extremes (Marra et al., 2018; Zorzetto et al., 2016). Events generated by different types of processes and thus described by distinct distributions, such as

midlatitude versus tropical cyclones (or, in our case, *Type-1* vs. *Type-2*), can be combined to derive a compound distribution for extreme return levels (Marra, Zoccatelli, et al., 2019; Miniussi et al., 2020). This distribution quantifies the yearly exceedance probability ζ associated with the precipitation amount x as a function of the intensity distributions of the ordinary events ($F_{i=1,\dots,S}$, where i represents the type of process) and the expected value of their yearly number of occurrences (n_i) such that $\zeta(x) \approx F_1^{n_1} \cdot F_2^{n_2} \cdot \dots \cdot F_S^{n_S}$ (Marra, Zoccatelli, et al., 2019). In this framework, changes in extreme return levels can be expressed as functions of the projected changes in the intensity distributions of the ordinary events and in the expected value of their yearly occurrences. While the occurrence frequency of synoptic events in the region can be resolved by ESMS (Cavicchia et al., 2020; Hochman, Harpaz, et al., 2018), precipitation intensity requires information on two degrees of freedom (i.e., the two parameters describing the distribution).

3.1. Ordinary Events Distributions and Return Levels

Ordinary events are defined as nonzero (i.e., ≥ 0.1 mm) daily precipitation amounts (Zorzetto et al., 2016) associated with a precipitation type based on a semiautomatic, daily-based, synoptic classification (Alpert et al., 2004). Wet days corresponding to systems that are expected to be dry may have been wrongly classified; for example, synoptic conditions in the aftermath of Mediterranean cyclones are easily misinterpreted by the semiautomatic method. These were individually examined and labeled as *Type-1* if occurring up to 2 days after a *Type-1* day and as *Type-2* in the remaining cases (Table S1).

Previous studies show that a Weibull distribution (stretched-exponential) in the form $F(x; \lambda, \kappa) = 1 - e^{-(x/\lambda)^\kappa}$, where λ is the scale and κ the shape parameter, well describes the tail of the two types of ordinary events in the region (Marra, Zoccatelli, et al., 2019). The shape parameter determines the tail heaviness, with heavier tails for smaller shapes and vice versa. These parameters are estimated left-censoring the lowest 75% of the observations while keeping their weight in probability, and using a least squares linear regression in Weibull-transformed coordinates (Marra, Zoccatelli, et al., 2019). The left-censoring prevents contaminations from the lower tail of the distribution, which may require more general formulations (Cavanaugh et al., 2015; Papalexou et al., 2018) and is sensitive to the accuracy of the measurement device (Marra, Zoccatelli, et al., 2019). After left-censoring, the number of data points used for the parameter estimation in each of the stations is 426 ± 175 for *Type-1* (minimum 66), and 153 ± 68 (minimum 30) for *Type-2*. The expected number of yearly ordinary events is computed, for each type, as the mean of the yearly number of wet days. Extreme return levels are computed numerically by inverting the formulation $\zeta(x) \approx F_1^{n_1} \cdot F_2^{n_2}$. Sample uncertainty in parameters and return levels is quantified via bootstrap with replacement (10^3 repetitions) among the years in the record (Overeem et al., 2008). The resulting return levels (Figures 1 and S2) are consistent with traditional methods based on the observed annual maxima (Figure S3) but have significantly smaller uncertainty (22%, as opposed to 39%, median uncertainty on 100-year return levels).

3.2. Local Constraints of the Intensity Distributions

A functional relationship between the scale λ and shape κ parameter of the ordinary events distributions would reduce the representation of precipitation intensity to one degree of freedom, enabling us to provide projections of extremes based only on changes in the mean intensity of ordinary events. The significance of the relationship between the parameters describing the two types of ordinary events at each of the five groups of stations is tested using the rank correlation (10^4 Monte Carlo reshuffling realizations). The coefficient α of the relations in the form $\kappa = \alpha \cdot \log \lambda + C$ is derived for each of the five groups and the two event types using a linear regression model based on a χ^2 minimization and considering parameter estimation errors in a Monte Carlo framework (10^3 realizations).

The coefficients α , calculated for each group, represent the local constraints on the intensity distribution. Higher α implies a stronger decrease in tail heaviness in response to an increase in the median intensity and vice versa. Under these constraints, the distribution has one degree of freedom, meaning that any quantity not orthogonal to the constraint (e.g., mean, median, and standard deviation) is sufficient to describe the distribution. Here, we use the median intensity, hereon denoted I , as it is less sensitive than the mean to

the stochastic uncertainty in the realization of extremes: $F_i(x; \lambda_i, \kappa_i) = F(x; I_i)$. The return level x associated with the yearly exceedance probability p can be written as a function of median intensity and expected number of yearly occurrences of the two types of ordinary events by inverting the extreme value distribution $\zeta(x)$: $x(p) = \zeta^{(-1)}(p; I_1, n_1; I_2, n_2)$.

We assume that temporal changes in the distribution of ordinary events will preserve these local observational constraints. This resembles the assumptions behind regionalization approaches in which spatial information is traded for record length (Buishand, 1991) but extends its meaning in that (i) temporal changes are allowed and (ii) the information on the interaction between precipitating systems and local features provided by each individual station is fully exploited (e.g., Marra, Armon, et al., 2020). To support our assumption, we test the significance of the constraints in historical observations in a Monte Carlo framework by examining groups of nonconsecutive years with consistently different median intensity (see Figure S4) along the following steps: (1) at each station and precipitation type, years are ranked according to the median ordinary events intensity; (2) six 5-year subsets of nonconsecutive years are created by selecting three groups (15 years) from the largest intensity years and three from the smallest intensity; (3) Weibull parameters are estimated at each station for the 5-year subsets; (4) 10^3 m -elements synthetic samples, where m is the number of wet days in the observed 5-year subsets, are generated according to the obtained distributions and the parameters describing the samples are estimated to quantify the impact of parameter estimation uncertainty; (5) logarithmic relations between the parameter pairs are derived for each subset; and (6) the α coefficient representing the local constraint is compared to the distribution of coefficients of the logarithmic relations at (5).

3.3. Climate Projections

Projected changes in median intensity and expected number of yearly occurrences of the two precipitation types are obtained by examining the difference between the ends of the 21st century (~ 2080 – 2100) and the 20th century (~ 1980 – 2005) under the RCP8.5 emission scenario (Riahi et al., 2011). We estimated these differences using the data presented in Hochman, Harpaz, et al. (2018) and Zappa et al. (2015), calculated for 8 and 17 CMIP5 models, respectively. We choose the changes in occurrence and median intensities from these two studies, as they are produced for the desired time period and emission scenario, and because these parameters are considered more robust than the changes in extremes that can be derived from the CMIP5 models themselves (Fatichi et al., 2016). In particular, the changes in synoptic circulation over the study region derived from CMIP5 ensembles were shown to be consistent among models (Hochman, Harpaz, et al., 2018; Zappa et al., 2015).

The acquired changes we used are as follows—*Type-1*: expected number of yearly occurrence is projected to decrease by 15%–35% ($-25\% \pm 10\%$); median intensity is projected to decrease by 20%–25% ($-22.5\% \pm 5\%$); *Type-2*: expected number of yearly occurrence is projected to increase by 13% ($+13\% \pm 5\%$); annual *Type-2* precipitation amounts are projected to remain unchanged, which leads to a 12% decrease in the median intensity ($-12\% \pm 5\%$). These numbers result in a 20%–30% decrease in mean annual precipitation, which is consistent with the AR5 IPCC report (IPCC, 2014). As based on relative differences between historic and future simulations, we expect these projections to be less sensitive to systematic biases in the quantification of wet days from CMIP5 models (e.g., too many drizzle days).

Changes in extreme return levels are computed in a Monte Carlo framework considering uncertainties in the projections and in the local constraints (i.e., the α coefficients), as follows. At each station, 10^3 projections are created by (1) sampling the projected change in number and median intensity of the two ordinary events types from normal distributions and (2) sampling the α coefficient of the local constraint relations from the Monte Carlo realizations. Note that, since the ratio between median and mean of Weibull distributions smoothly depends on the shape parameter κ and is independent from the scale λ , for the changes in shape observed in this study, one can safely assume a one-to-one correspondence between projected changes in the mean and in the median (e.g., the difference between percent change in the mean and percent change in the median is smaller than the uncertainties on the projections themselves). This is useful

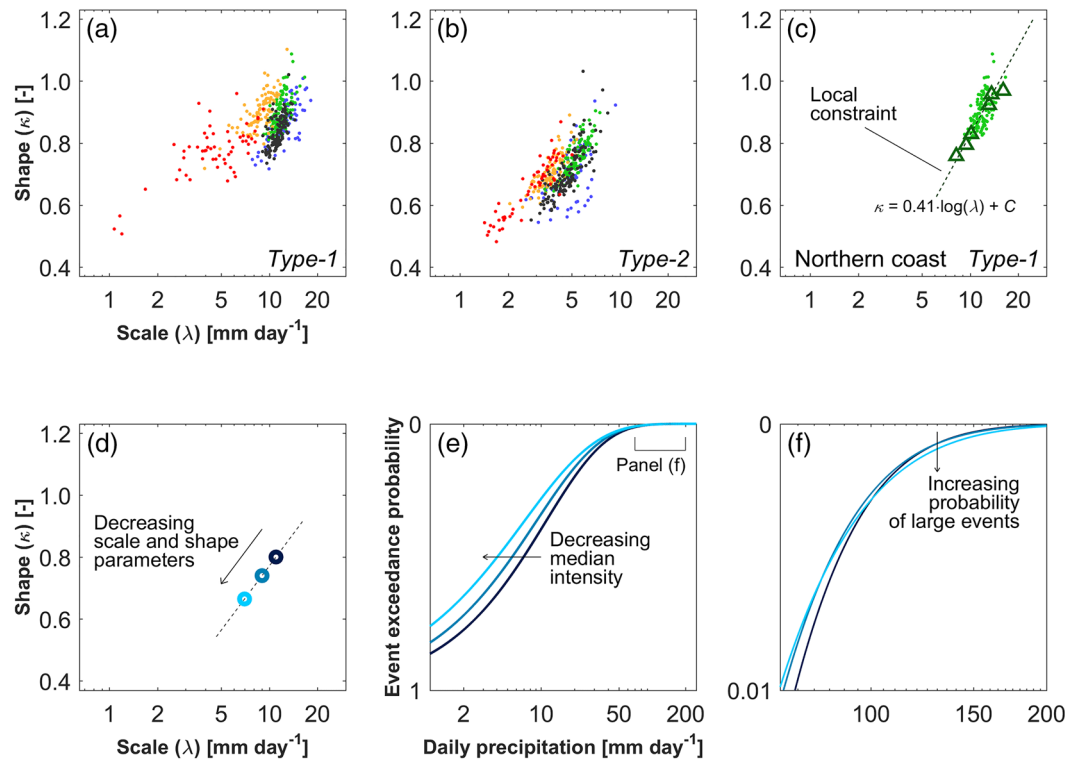


Figure 2. Local constraints on the intensity distribution of ordinary precipitating events. (a, b) Scatter plots of the shape (κ) and scale (λ) parameters of the observed distributions for the two types of ordinary events; colors refer to the five groups of stations as in Figure 1a. (c) Example of the local constraint (Type-1, northern coast); triangles represent the median (among stations) parameters obtained in the split-sample test using, for each station, groups of five nonconsecutive years with increasing median intensity of the ordinary events; triangles thus represent historical variations of intensity. Local constraints for all cases are shown in Figure S4. (d) Schematic of the projection of changes in the intensity distribution of the ordinary events along the constraints ($\alpha = 0.3$, $\lambda = 11.0, 9.0, 7.0$ mm day⁻¹, and $\kappa = 0.8, 0.74, 0.66$; black, blue, and cyan, respectively); (e) event exceedance probability distributions associated with the three pairs of scale and shape parameters shown in (d); and (f) the largest 1% of the events in these distributions.

since the median is a better descriptor for observed data, whereas the mean is commonly provided by ESMs output.

4. Application to the South-Eastern Mediterranean

4.1. Local Constraints on the Distribution of Ordinary Events

While relations between scale λ and shape κ parameters of the ordinary events distributions are not expected a priori, statistically significant relations ($>3\sigma$ significance level) are found for the given data when focusing on local groups of stations in which distinct local features dominate the interactions with precipitation systems (Figures 2a–2c and S4). Functional dependence of the form $\kappa = \alpha \cdot \log \lambda + C$, where α and C are empirically determined, was found to approximate these relations in each group, generally explaining most of the observed variance (Figure S4). The hypothesis of a local constraint α being significantly different from the coefficients obtained from temporally splitting the records is rejected in all the cases (5% significance level). Thus, the local values of α indeed reflect historical changes in the median intensity of ordinary events at each station, supporting the validity of the approach under changing conditions (Figures 2c and S4). It is worth noting that these relations are based on historical observations and thus comprise observed changes in both dynamics and thermodynamics.

The observed constraints imply that changes in the median intensity are linked to contrasting changes in extremes, that is, decreasing median intensity decreases the precipitation amount yielded by typical ordinary

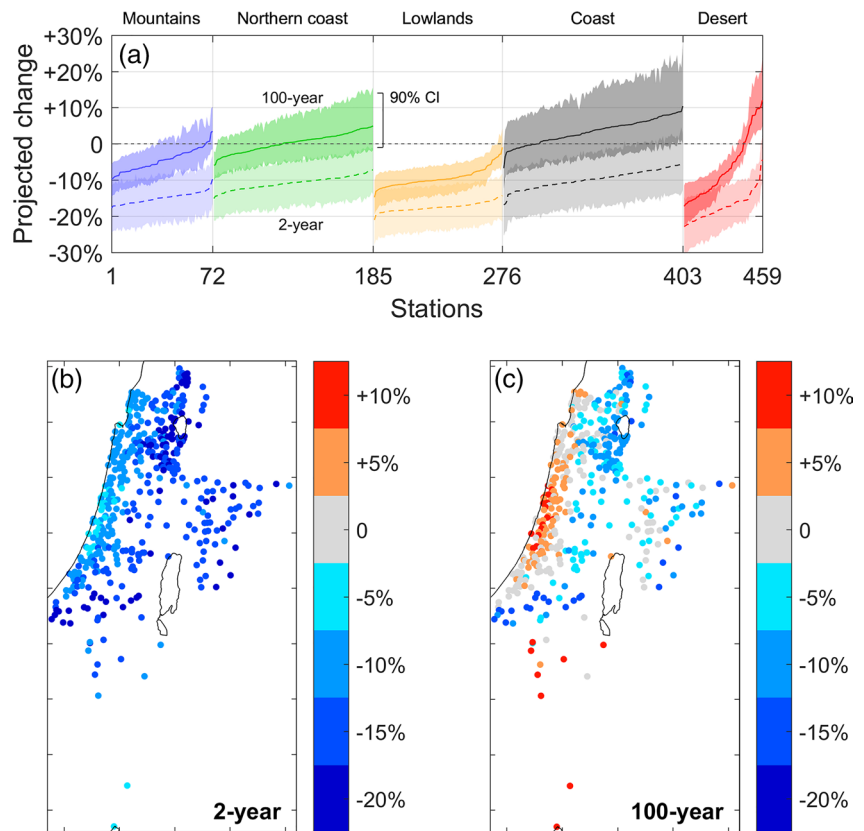


Figure 3. Projected changes in 2-year and 100-year return levels (50% and 1% yearly exceedance probability, respectively) for the end of the century (difference between ~2080–2100 and ~1980–2005) under the RCP8.5 emission scenario. (a) Distribution of the projected change and relative uncertainty (90% confidence interval considering uncertainties both in climate projections and local constraints) shown as transposed cumulative distributions; colors refer to the five groups of stations as in Figure 1a. (b, c) Map of the projected changes for the 2-year (b) and 100-year (c) return levels.

events (Figures 2d and 2e) but increases the probability associated with the largest events and vice versa (Figure 2f). This counterintuitive behavior is consistent with previous theory and observations of extreme precipitation and supports the local constraints approach as a framework for quantifying changes in extremes (Myhre et al., 2019; O’Gorman & Schneider, 2009; Pendergrass, 2018; Pendergrass & Knutti, 2018; Wasko et al., 2018).

4.2. Projections of Future Extremes

The sensitivity of extreme return levels to changes in the ordinary events (Figures S5 and S6) highlights that different return levels can have different responses and that the local sensitivities associated with each event type can differ significantly. For example, in most of the region, return levels are tied to changes in intensity and number of *Type-1* events, while changes in *Type-2* are crucial drivers for extreme return levels in the desert areas (Figure S5). Local changes in extreme return levels are thus related to mean (or median) changes in precipitation in a complex manner.

The projected changes in occurrence frequency of the two types (25% decrease and 13% increase, respectively) and intensity (20%–25% and 12% decrease, respectively) yield the changes in the extreme return levels shown in Figure 3 (see Figure S7 for more details). An overall 5%–20% decrease of the 2-year return levels is seen, driven by the decrease in the occurrence frequency of Mediterranean cyclones and in the median intensity of both types of systems. Since in the climatological setting of the region, 2-year return levels roughly correspond to 99th wet-day percentiles, this is consistent with previous results based on downscaling methods (Hochman, Mercogliano, et al., 2018). The picture is drastically different for the 100-year return levels

which could not be assessed in previous studies. Along the coast and in the southern desert, the negative sensitivity to changes in the median intensity (Figures S5 and S6) dominates, and the rarest extremes are projected to increase, consistently with Figure 2f. These results imply two adverse effects: (i) amplified water scarcity and reduced flood and landslide risks in most of the region (Alpert et al., 2002; Peleg et al., 2015; Samuels et al., 2009) and (ii) increased intensity of the most severe events along the coast and southern deserts, associated with augmented risk of extreme pluvial flooding in coastal cities, and of flash floods, debris flows and geomorphic responses in the southern deserts (Rinat et al., 2020; Shmilovitz et al., 2020).

5. Discussion and Conclusions

In the south-eastern Mediterranean, the dominance of two precipitating systems and the availability of high-density local data makes it possible to simplify the statistical description of ordinary precipitation events, and therefore of extreme events that emerge as the tails of their distributions. Previous studies on the water resources of the region projected a “less rainfall, more extremes” situation, with increased extremes insufficient to impact water resources in generally drying conditions. However, these previous studies could not quantify changes in extreme return levels and therefore risk (Alpert et al., 2002; Peleg et al., 2015). Combining information on the occurrence frequency and intensity of the two dominant precipitation types from ESM projections and observational constraints from rain stations, we show that the changes in extreme return levels strictly depend on the sought probability. A tendency toward a general decrease in the intensity of the 2-year events is found, together with an increase of the most severe (100-years) events along the coast and in the desert areas.

The consistency of the synoptic variations in the RCP8.5 scenario in the region (Hochman, Harpaz, et al., 2018; Zappa et al., 2015) and of the local constraints (Figure S6) demonstrate the reliability of the proposed approach and the local projected response. Nevertheless, our predictions may be refined by analyzing additional scenarios and local data. It is plausible that similar improvements in the projection of extremes can be made in other regions, even though projected changes in the synoptic circulation systems might be less robust (Shepherd, 2014), calling for specific efforts to narrow this source of uncertainty. Our results rely on the hypothesis that future changes in the distribution of ordinary events will preserve local observational constraints. Future convection-permitting model runs could help validate this hypothesis or suggest alternative constraints. In fact, future climate might reach some tipping point after which the observational local constraints may no longer hold. For example, new synoptic systems could be introduced in the region (such as tropical-like cyclones), or the track of existing systems could change to such a degree that the interactions with local features might change substantially, thus deviating from the observed constraints (e.g., northward shift of Mediterranean cyclones track). Our results, which pertain to daily precipitation, assume no change in the spatial structure of precipitation events at scales smaller than the resolutions of the used climate models. Improvements in the statistical description of the precipitating systems at multiple temporal and spatial scales derived from observations and/or convection-permitting models could fill this gap by quantifying their structural response to external forcing (Cannon & Innocenti, 2019; Chen et al., 2020; Marra, Borga, et al., 2020; Peleg et al., 2018; Wasko et al., 2016).

In contrast to traditional methods, the local constraints approach does not require long records; rather, it only requires local observations of ordinary events to constrain the intensity distributions. To this end, future work should address whether a similar methodology can be applied using remotely sensed precipitation as opposed to rain gauges, which would allow this technique to be applied in many ungauged locations of the Earth (Marra, Nikolopoulos, et al., 2019). While uncertainty in ESMs remains a significant challenge to the community (Palmer & Stevens, 2019), our results point to increased investment in local measurements as an actionable and promising path to reduced uncertainty in the projection of extremes, independent of climate modeling efforts.

The framework can be extended to other processes whose extremes emerge from underlying distributions of ordinary events, such as extremes emerging from the combination of different physical phenomena, for example, winds and storm surges from different types of cyclones (Cavicchia et al., 2020; Miniussi et al., 2020). Similarly, it can be applied to phenomena whose intensity and occurrence may change independently, for example, occurrence and maximum lifetime intensity of tropical cyclones (Knutson et al., 2010) or precipitation in many areas (Markonis et al., 2019; Papalexiou & Montanari, 2019). In regions where local

constraints can be obtained, the approach proposed here can improve the predictability of climate change impact on extremes at scales relevant for impact studies, whose uncertainty was previously considered irreducible due to modeling uncertainty and natural variability.

Data Availability Statement

Precipitation data were provided by Israel Meteorological Service (<https://ims.gov.il/en>, September 2018; data are freely available in Hebrew only) and Ministry of Water and Irrigation of Jordan, Technical Affairs, Studies Directorate, Hydrological and Meteorological Information Systems (rainfall stations archives files, October 2018; available upon request to the data providers). Data and codes supporting the results are available at: <https://doi.org/10.5281/zenodo.4286160> and <https://doi.org/10.5281/zenodo.3971558>. The linear fit with uncertainty in x and y was performed based on the function by J. Browaeys, MATLAB Central File Exchange (<https://www.mathworks.com/matlabcentral/fileexchange/45711-linear-fit-with-both-uncertainties-in-x-and-in-y>, retrieved March 25, 2020).

Acknowledgments

The authors declare no conflict of interests. The authors thank Prof. Pinhas Alpert for the synoptic classification. This study was funded by the Israel Ministry of Science and Technology (grant no. 61792), Israel Science Foundation (grant no. 1069/18), NSF-BSF (grant no. BSF 2016953), JNF (grant no. 90-01-550-18), and Google (gift grant). It is a contribution to the HyMeX program.

References

- Alpert, P., Ben-Gai, T., Baharad, A., Benjamini, Y., Yekutieli, D., Colacino, M., et al. (2002). The paradoxical increase of Mediterranean extreme daily rainfall in spite of decrease in total values. *Geophysical Research Letters*, 29(11), 1536. <https://doi.org/10.1029/2001GL013554>
- Alpert, P., Osetinsky, I., Ziv, B., & Shafir, H. (2004). Semi-objective classification for daily synoptic systems: Application to the Eastern Mediterranean climate change. *International Journal of Climatology*, 24(8), 1001–1011.
- Armon, M., Dente, E., Smith, J. A., Enzel, Y., & Morin, E. (2018). Synoptic-scale control over modern rainfall and flood patterns in the levant drylands with implications for past climates. *Journal of Hydrometeorology*, 19, 1077–1096.
- Blöschl, G., Bierkens, M. F. P., Chambel, A., Cudennec, C., Destouni, G., Fiori, A., et al. (2019). Twenty-three unsolved problems in hydrology (UPH)—A community perspective. *Hydrological Sciences Journal*, 64(10), 1141–1158.
- Buishand, T. A. (1991). Extreme rainfall estimation by combining data from several sites. *Hydrological Sciences Journal*, 36(4), 345–365. <https://doi.org/10.1080/0262666910949251>
- Calinski, T., & Harabasz, J. A. (1974). A dendrite method for cluster analysis. *Communications in Statistics*, 3(1), 1–27.
- Cannon, A. J., & Innocenti, S. (2019). Projected intensification of sub-daily and daily rainfall extremes in convection-permitting climate model simulations over North America: Implications for future intensity–duration–frequency curves. *Natural Hazards and Earth System Sciences*, 19, 421–440.
- Cavanaugh, N. R., Gershunov, A., Panorska, A. K., & Kozubowski, T. J. (2015). The probability distribution of intense daily precipitation. *Geophysical Research Letters*, 42, 1560–1567. <https://doi.org/10.1002/2015GL063238>
- Cavicchia, L., Peplar, A., Dowdy, A., Evans, J., Di Luca, A., & Walsh, K. (2020). Future changes in the occurrence of hybrid cyclones: The added value of cyclone classification for the east Australian low-pressure systems. *Geophysical Research Letters*, 47, e2019GL085751. <https://doi.org/10.1029/2019GL085751>
- Ceola, S., Laio, F., & Montanari, A. (2014). Satellite nighttime lights reveal increasing human exposure to floods worldwide. *Geophysical Research Letters*, 41, 7184–7190. <https://doi.org/10.1002/2014GL061859>
- Chen, Y., Paschalis, A., Kendon, E., Kim, D., & Onof, C. (2020). Changing spatial structure of summer heavy rainfall, using convection-permitting ensemble. *Geophysical Research Letters*, 48, e2020GL090903. <https://doi.org/10.1029/2020GL090903>
- Chow, V. T., Maidment, D. R., & Mays, L. W. (1988). *Applied hydrology*. McGraw-Hill.
- Coles, S. (2001). *An introduction to statistical modeling of extreme values*. London: Springer-Verlag.
- Diskin, M. H. (1970). Factors affecting variations of mean annual rainfall in Israel. *International Association of Scientific Hydrology Bulletin*, 15(4), 41–49.
- Fatichi, S., Ivanov, V. Y., Paschalis, A., Peleg, N., Molnar, P., Rimkus, S., et al. (2016). Uncertainty partition challenges the predictability of vital details of climate change. *Earth's Future*, 4, 240–251. <https://doi.org/10.1002/2015EF000336>
- Fischer, E. M., Beyerle, U., & Knutti, R. (2013). Robust spatially aggregated projections of climate extremes. *Nature Climate Change*, 3, 1033–1038.
- Fischer, E. M., & Knutti, R. (2016). Observed heavy precipitation increase confirms theory and early models. *Nature Climate Change*, 6, 986–991.
- Fosser, G., Kendon, E. J., Stephenson, D., & Tucker, S. (2020). Convection-permitting models offer promise of more certain extreme rainfall projections. *Geophysical Research Letters*, 47, e2020GL088151. <https://doi.org/10.1029/2020GL088151>
- Giorgi, F. (2006). Climate change hot-spots. *Geophysical Research Letters*, 33, L08707. <https://doi.org/10.1029/2006GL025734>
- Hausfather, Z., Drake, H. F., Abbot, T., & Schmidt, G. A. (2019). Evaluating the performance of past climate model projections. *Geophysical Research Letters*, 47, e2019GL085378. <https://doi.org/10.1029/2019GL085378>
- Hochman, A., Harpaz, T., Saaroni, H., & Alpert, P. (2018). Synoptic classification in 21st century CMIP5 predictions over the Eastern Mediterranean with focus on cyclones. *International Journal of Climatology*, 38, 1476–1483.
- Hochman, A., Mercogliano, P., Alpert, P., Saaroni, H., & Bucchignani, E. (2018). High-resolution projection of climate change and extremity over Israel using COSMO-CLM. *International Journal of Climatology*, 38(14), 5095–5106.
- IPCC. (2014). In Core Writing Team, R. K. Pachauri & L. A. Meyer (Eds.), *Climate change 2014: Synthesis report. Contribution of working groups I, II and III to the fifth assessment report of the Intergovernmental Panel on Climate Change*. Geneva, Switzerland: IPCC.
- Kelder, T., Muller, M., Slater, L. J., Marjoribanks, T. I., Wilby, R. L., Prudhomme, C., et al. (2020). Using UNSEEN trends to detect decadal changes in 100-year precipitation extremes. *Npj Climate and Atmospheric Sciences*, (3), 47.
- Keller, M., Kroner, N., Fuhrer, O., Luthi, D., Schmidli, J., Stengel, M., et al. (2018). The sensitivity of alpine summer convection to surrogate climate change: An intercomparison between convection-parameterizing and convection-resolving models. *Atmospheric Chemistry and Physics*, 18(8), 5253–5264.

- Kendon, E. J., Roberts, N. M., Fowler, H. J., Roberts, M. J., Chan, S. C., & Senior, C. A. (2014). Heavier summer downpours with climate change revealed by weather forecast resolution model. *Nature Climate Change*, *4*, 570–576.
- Knutson, T. R., McBride, J. L., Chan, J., Emanuel, K., Holland, G., Landsea, C., et al. (2010). Tropical cyclones and climate change. *Nature Geoscience*, *3*, 157–163.
- Marani, M., & Ignaccolo, M. (2015). A metastatistical approach to rainfall extremes. *Advances in Water Resources*, *79*, 121–126.
- Markonis, Y., Papalexiou, S. M., Martinkova, M., & Hanel, M. (2019). Assessment of water cycle intensification over land using a multisource global gridded precipitation dataset. *Journal of Geophysical Research: Atmospheres*, *124*, 11175–11187. <https://doi.org/10.1029/2019JD030855>
- Marra, F., Armon, M., Borga, M., & Morin, E. (2021). Orographic effect on extreme precipitation statistics peaks at hourly time scales. *Geophysical Research Letters*, e2020GL091498. <https://doi.org/10.1029/2020GL091498>
- Marra, F., Borga, M., & Morin, E. (2020). A unified framework for extreme subdaily precipitation frequency analyses based on ordinary events. *Geophysical Research Letters*, *47*, e2020GL090209. <https://doi.org/10.1029/2020GL090209>
- Marra, F., Nikolopoulos, E. I., Anagnostou, E. N., Bárdossy, A., & Morin, E. (2019). Precipitation frequency analysis from remotely sensed datasets: A focused review. *Journal of Hydrology*, *574*, 699–705.
- Marra, F., Nikolopoulos, E. I., Anagnostou, E. N., & Morin, E. (2018). Metastatistical Extreme Value analysis of hourly rainfall from short records: Estimation of high quantiles and impact of measurement errors. *Advances in Water Resources*, *117*, 27–39.
- Marra, F., Zoccatelli, D., Armon, M., & Morin, E. (2019). A simplified MEV formulation to model extremes emerging from multiple non-stationary underlying processes. *Advances in Water Resources*, *127*, 280–290.
- Miniussi, A., Villarini, G., & Marani, M. (2020). Analyses through the Metastatistical Extreme Value distribution identify contributions of Tropical Cyclones to rainfall extremes in the Eastern United States. *Geophysical Research Letters*, *47*, e2020GL087238. <https://doi.org/10.1029/2020GL087238>
- Myhre, G., Alterskjær, K., Stjern, C. W., Hodnebrog, Ø., Marelle, L., Samset, B. H., et al. (2019). Frequency of extreme precipitation increases extensively with event rareness under global warming. *Scientific Reports*, *9*, 16063.
- NOAA. (2020). *U.S. billion-dollar weather and climate disasters*. NCEI. <https://www.ncdc.noaa.gov/billions/summary-stats>
- O’Gorman, P. A., & Schneider, T. (2009). The physical basis for increases in precipitation extremes in simulations of 21st-century climate change. *Proceedings of the National Academy of Sciences of the United States of America*, *106*(35), 14773–14777.
- Overeem, A., Buishand, A., & Holleman, I. (2008). Rainfall depth-duration-frequency curves and their uncertainties. *Journal of Hydrology*, *348*, 124–134.
- Palmer, T., & Stevens, B. (2019). The scientific challenge of understanding and estimating climate change. *Proceedings of the National Academy of Sciences of the United States of America*, *116*(49), 24390–24395.
- Papalexiou, S. M., AghaKouchak, A., & Fofoula-Georgiou, E. (2018). A diagnostic framework for understanding climatology of tails of hourly precipitation extremes in the United States. *Water Resources Research*, *54*, 6725–6738. <https://doi.org/10.1029/2018WR022732>
- Papalexiou, S. M., & Montanari, A. (2019). Global and regional increase of precipitation extremes under global warming. *Water Resources Research*, *55*, 4901–4914. <https://doi.org/10.1029/2018WR024067>
- Paprotny, D., Sebastian, A., Morales-Napoles, O., & Jonkman, S. N. (2018). Trends in flood losses in Europe over the past 150 years. *Nature Communications*, *9*, 1985.
- Peleg, N., Marra, F., Faticchi, S., Molnar, P., Morin, E., Sharma, A., & Burlando, P. (2018). Intensification of convective rain cells at warmer temperatures observed from high-resolution weather radar data. *Journal of Hydrometeorology*, *19*, 715–726.
- Peleg, N., Shamir, E., Georgakakos, K. P., & Morin, E. (2015). A framework for assessing hydrological regime sensitivity to climate change in a convective rainfall environment: A case study of two medium-sized eastern Mediterranean catchments, Israel. *Hydrology and Earth System Sciences*, *19*, 567–581.
- Pendergrass, A. G. (2018). What precipitation is extreme? *Science*, *360*, 6393.
- Pendergrass, A. G., & Knutti, R. (2018). The uneven nature of daily precipitation and its change. *Geophysical Research Letters*, *45*, 11980–11988. <https://doi.org/10.1029/2018GL080298>
- Pfahl, S., O’Gorman, P. A., & Fischer, E. M. (2017). Understanding the regional pattern of projected future changes in extreme precipitation. *Nature Climate Change*, *7*, 423–428.
- Phillips, P., & Perron, P. (1988). Testing for a unit root in time series regression. *Biometrika*, *75*, 335–346.
- Prein, A. F., Rasmussen, R., Castro, C. L., Dai, A., & Minder, J. (2020). Special issue: Advances in convection permitting climate modeling. *Climate Dynamics*(55), 1–2.
- Riahi, K., Rao, S., Krey, V., Cho, C., Chirkov, V., Fischer, G., et al. (2011). RCP 8.5—A scenario of comparatively high greenhouse gas emissions. *Climatic Change*, *109*, 33–57.
- Rinat, Y., Marra, F., Armon, M., Metzger, A., Levi, Y., Khain, P., et al. (2021). Hydrometeorological analysis and forecasting of a 3-day flash-flood-triggering desert rainstorm. *Natural Hazards and Earth System Sciences*. In press. <https://doi.org/10.5194/nhess-2020-189>
- Samuels, R., Rimmer, A., & Alpert, P. (2009). Effect of extreme rainfall events on the water resources of the Jordan River. *Journal of Hydrology*, *375*, 513–523.
- Serinaldi, F., & Kilsby, C. G. (2015). Stationarity is undead: Uncertainty dominates the distribution of extremes. *Advances in Water Resources*, *77*, 17–36.
- Shepherd, T. G. (2014). Atmospheric circulation as a source of uncertainty in climate change projections. *Nature Geoscience*, *7*, 703–708.
- Shmilovitz, Y., Morin, E., Rinat, Y., Haviv, I., Carmi, G., Mushkin, A., & Enzel, Y. (2020). Linking frequency of rainstorms, runoff generation and sediment transport across hyperarid talus-pediment slopes. *Earth Surface Processes and Landforms*, *49*(7), 1644–1659.
- Sippel, S., Mitchell, D., Black, M. T., Dittus, A. J., Harrington, L., Schaller, N., & Otto, F. E. L. (2015). Combining large model ensembles with extreme value statistics to improve attribution statements of rare events. *Weather and Climate Extremes*, *9*, 25–35.
- Tabari, H. (2021). Extreme value analysis dilemma for climate change impact assessment on global flood and extreme precipitation. *Journal of Hydrology*, *593*, 125932.
- Wasko, C., Lu, W. T., & Mehrotra, R. (2018). Relationship of extreme precipitation, dry-bulb temperature, and dew point temperature across Australia. *Environmental Research Letters*, *13*, 074031.
- Wasko, C., Sharma, A., & Westra, S. (2016). Reduced spatial extent of extreme storms at higher temperatures. *Geophysical Research Letters*, *43*, 4026–4032. <https://doi.org/10.1002/2016GL068509>
- Wilcox, E. M., & Donner, L. J. (2007). The frequency of extreme rain events in satellite rain-rate estimates and an atmospheric general circulation model. *Journal of Climate*, *20*, 53–69.
- Winsemius, H. C., Aerts, J. C. J. H., van Beek, L. P. H., Bierkens, M. F. P., Bouwman, A., Jongman, B., et al. (2016). Global drivers of future river flood risk. *Nature Climate Change*, *6*, 381–385.

- Zappa, G., Hawcroft, M. K., Shaffrey, L., Black, E., & Brayshaw, D. J. (2015). Extratropical cyclones and the projected decline of winter Mediterranean precipitation in the CMIP5 models. *Climate Dynamics*, *45*(7–8), 1727–1738.
- Zorzetto, E., Botter, G., & Marani, M. (2016). On the emergence of rainfall extremes from ordinary events. *Geophysical Research Letters*, *43*, 8076–8082. <https://doi.org/10.1002/2016GL069445>

References From the Supporting Information

- Alpert, P., Osetinsky, I., Ziv, B., & Shafir, H. (2004). Semi-objective classification for daily synoptic systems: Application to the eastern Mediterranean climate change. *International Journal of Climatology*, *24*(8), 1001–1011.
- Hosking, J. R. M. (1990). L-moments: Analysis and estimation of distributions using linear combinations of order statistics. *Journal of the Royal Statistical Society, Series B (Methodological)*, *52*(1), 105–124.